# THE SPECTRAL REFLECTANCE OF SHIP WAKES BETWEEN 400 AND 900 NANOMETERS

*Robert Wright[1], Justin Deloatch[2], Stephanie Osgood[2], and Jinchun Yuan[2]*
1. Hawai'i Institute of Geophysics and Planetology, University of Hawai'i at Mānoa, Honolulu, HI, U.S.A.
2. School of Mathematics, Science, and Technology, Elizabeth State University, Elizabeth City, NC, U.S.A.

*Abstract* — **This technical note describes the use of an airborne hyperspectral imaging sensor (HICO – Hyperspectral Imager of the Coastal Ocean) to record the spectral reflectance characteristics of centerline ship wakes in the 400 to 900 nm wavelength region. Data were collected for a target of known provenance (the United States Coast Guard Cutter Kittiwake) off the Wai'anae coast of O'ahu, Hawai'i, on 8 April 2010. HICO acquired data in 60 spectral bands by flying along the long axis of the wake while the vessel travelled at three speeds (~3.6 m $s^{-1}$ or 7 knots; ~7.2 m $s^{-1}$ or 14 knots; and ~11.2 m $s^{-1}$ or 21 knots). A flying altitude of ~1500 m yielded a spatial resolution of ~1.5 m. Spectral profiles along and across the wake axes are presented which show how the spectral reflectance of the centerline wake varies spatially and temporally as a function of vessel speed. Length (and to a lesser extent, width) vary in proportion to speed. In common with previous studies and model predictions, the wakes show a pronounced greening of the wake (i.e. enhanced reflectance at ~550 nm), with evidence for elevated reflectance at 750–800 nm. Resampling the data from its raw 1.5 m spatial resolution yields insights into how the turbulent wake becomes spectrally inseparable from the background water as spatial resolution decreases (i.e. becomes increasingly coarse). Using a simple statistical test, the wake becomes spectrally similar to the background ocean as the resolution approaches 60 m.**

**Keywords: Remote sensing, Spectral reflectance, Ship wakes**

## I. INTRODUCTION

When a ship moves through water it disturbs the upper reaches of the water column generating a wake. The wakes are persistent in time, and constitute a spatial fingerprint for the passage of a vessel which is far larger than the vessel itself which provide a target for detection and tracking of ships in maritime domain. The manifestation of ship wakes in synthetic aperture radar images has been well documented (e.g. Eldhuset, 1996; Hennings et al., 1999; Reed and Milgram, 2002), while their appearance in thermal infrared data has also been reported (McGlynn et al., 1990). Ship wakes can also manifest themselves as sunglitter anomalies, due to specular reflectance of sunlight from the facets of wake–generated waves (Munk et al., 1987). Less attention has been paid to the reflectance characteristics of ship wakes at visible and infrared wavelengths, the work of Zhang et al. (2004) being an important exception. The purpose of this technical note is to make a contribution to the literature in this regard, by presenting results that document the spectral reflectance characteristics of ship wakes between 400 and 900 nm, a spectral region in which Zhang et al. (2004) note that relatively few studies have documented wake properties.

A great deal of fundamental research has been conducted into the physics of wake generation (e.g. Thompson, 1887). A ship wake consists of two parts: the turbulent wake and the Kelvin wake (Figure 1b). The Kelvin wake is caused by waves emanating from the ship as it disturbs the water, and consists of two parts: divergent waves (the V–shaped feature apparent in Figure 1b) and transverse waves (approximately perpendicular to the direction of vessel motion and barely visible in Figure 1b). The wake is visible in optical remote sensing images because the tilted facets of the waves that comprise the wake act to specularly reflect light back to the sensor, appearing bright in such images (Munk et al., 1987).

The turbulent wake is relatively narrow and extends aft of the vessel (the bright, high reflectance feature visible in Figure 1 a, b, and c). The turbulent wake, rather than a sunglint anomaly, is a foam (i.e. large cavities of air separated by thin layers of liquid). The bubbles can be produced by a) entrainment of air at the water air interface as the vessel disturbs the water surface and b) propeller cavitation at higher vessel speeds (National Defense Research Committee, 1989). Light entering a foam is reflected and refracted at every bubble wall. The absorption of light as it passes through the bubble walls depends on the absorption coefficient of the liquid which form the bubble walls (spectrally dependent) and the wall thickness (i.e. the path length of the liquid that the photons must pass through). As light is only absorbed when passing through the absorbing medium a foam exhibits enhanced reflectance (when compared to a coherent body of the same liquid) as the amount of light absorbed at each thin bubble interface is relatively small, and at each interaction a proportion of light is backscattered towards the surface and ultimately to the sensor. Limited interaction of photons with the absorbing medium (thin bubble walls) before backscatter to the sensor means that the spectral absorption which imparts the liquid's color is suppressed, causing the foam to appear similarly (and highly) reflective at all visible wavelengths, thus appearing "white". As the foam dissipates (primarily as a result of dissolution; Trevorrow *et al*., 1994) the turbulent wake increasingly less visible as a reflectance anomaly with time since bubble formation (and hence distance from the point of generation, which is a function of vessel speed).

The purpose of this study is to make a contribution to the perceived gap in the literature noted by Zhang et al. (2004) by reporting the spectral reflectance of turbulent wakes in the visible and near-infrared, extracted from images of a vessel of known provenance acquired using an airborne hyperspectral imaging sensor.

## II. DATA AND METHODS

HICO (Hyperspectral Imager of the Coastal Ocean) acquires data in 60 spectral bands between 400 and 900 nm, at 12 bit radiometric resolution (i.e. 4095 distinct brightness levels). The data presented here were acquired from an altitude of ~1500 m, yielding a spatial resolution (pixel size) of ~1.5 m. To avoid sensor saturation over the highly reflective wake a neutral density filter was used to reduce light entering the instrument, while sensor integration time was also optimized to yield unsaturated measurements. The raw HICO data were calibrated (i.e. digital counts converted to spectral radiance) using a Sphere–Optics model SR–3A radiance calibration source, which uses tungsten and halogen lamps, and an integrating sphere, to provide a uniform light source between 300 and 1100 nm. Data were subsequently converted from at-sensor spectral radiance (W $m^{-2}$ $sr^{-1}$ $mm^{-1}$) to spectral reflectance (unitless) using the FLAASH algorithm (Fast Line–of–Sight Atmospheric Analysis of Spectral Hypercubes). FLAASH uses as its core the more widely known MODTRAN radiative transfer program (Berk et al., 1989). Atmospheric correction is essential given the strong scattering of blue light from the atmospheric column (upwelling radiance), which would otherwise strongly bias the raw radiance measurements to blue wavelengths.

An aim of the experiment was to assess the properties of the centerline wake generated by a vessel of known dimensions travelling at a range of speeds. Out target was the USGCG Kittiwake. The Kittiwake has a length of 27 m, a draft of 2 m, and two, one meter diameter, five bladed propellers. For 90 minutes the Kittiwake travelled a course similar in shape to a "running track" at three speeds for 15 minutes periods each, corresponding to the lower (3.6 m $s^{-1}$ or 7 knots), middle (7.2 m $s^{-1}$ or 14 knots) and upper range (~10.8 m $s^{-1}$ or 21 knots) of its speed limit. Flying overhead, HICO acquired images along the long axis of the wakes produced under each vessel speed condition, the aircraft maintaining a speed of close to 45 m $s^{-1}$ (100 m.p.h). Data were acquired between 13:15 and 14:45 Hawaiian Standard Time (UCT – 10 hours). During this time period wind speeds at sea level (recorded by NOAA's National Ocean Service Station NWWH1, located near Lihue, Kauai) varied between 4.6 and 5.9 m $s^{-1}$. Due to the unpredictable nature of the data collection process (occasional inability of the pilot to successfully align the aperture in the aircraft hull over the long axis of the wake; intermittent clouds; sunglint; imaging time lost whilst turning the aircraft) many of the images obtained during this interval were of limited value. The best three examples acquired at each vessel speed are shown in Figure 1. The spectral properties of the wakes apparent in these images are described in the next section.

## III. RESULTS AND DISCUSSION

Morphologically, the wakes generated by the Kittiwake change as vessel speed increases (Figure 1). Wake length increases with speed, as does wake width (although to a lesser degree). At 3.6 m $s^{-1}$ the turbulent wake is a single linear feature. At 7.2 and 10.8 m $s^{-1}$ the centerline wake splits into two lateral foam bands separated by a region of enhanced reflectance, this arrangement being most pronounced at the higher speed.

Figure 2 shows spectral reflectance profiles obtained for each of the three wakes shown in Figure 1. Figure 2a shows spectral reflectance of the centerline of the turbulent wake at 20 m increments aft of the vessel, terminating at the distance at which the wake was no longer visible in the image. Also shown for comparison, is the average spectral reflectance of adjacent open ocean. All data are plotted on the same scales to allow direct visual comparison of wake reflectance as a function of vessel speed.

The background ocean shows low reflectance at all wavelengths consistent with the high absorptance of water (the open water is in fact somewhat blue, but a very dark blue). Although nominally "white" the turbulent wakes do exhibit wavelength dependent spectral reflectance. The wake is significantly more reflective at all wavelengths than the background, with a peak in the visible green (~470–550 nm), decreasing towards the near–infrared. In each case (i.e. for each vessel speed) the same feature is observed, although it becomes increasingly more pronounced as vessel speed increases. In all cases spectral reflectance, and the visible green to near-infrared spectral slope, decrease with distance aft of the vessel, until the point is reached where the wake becomes spectrally indistinct from the background.

These results are consistent with previously published work. Greening of the wake spectrum was reported by Zhang et al. (2004). Although water scatters more strongly in the visible blue (molecular scattering from water molecules) the presence of bubbles (for which scattering efficiency increases with the –4/3 power of wavelength) causes enhanced reflectance at green wavelengths (Zhang et al., 2004).

The darkening of the spectral reflectance of the foam with wavelength between visible and near–infrared wavelengths has been observed before in studies of oceanic whitecap waves. In their analysis, Frouin et al. (1996) measured the reflectance of whitecaps between 440 nm and 1020 nm. They too found a pronounced decrease in reflectance from visible to near-infrared wavelengths, which contradicted earlier model predictions (Stabeno and Monahan, 1986) that foam reflectance should show no spectral dependence over this spectral interval.

Frouin et al. (1996) attribute this effect to the fact that the whitecap foam was in fact composed of two components: an upper layer of true foam (air bubbles with thin walls of water) overlying a sub–layer of water which contains bubble of air injected from above, but with a much lower bubble density (i.e. a higher water to air ratio). They postulate that enhanced absorption of light by this sub–layer produces the enhanced near–infrared absorption relative to visible wavelengths. The results presented here are consistent with this observation, due to the fact that the effect is more pronounced a) close to the vessel's stern and b) at higher vessel speeds. Frouin et al. (op. cit.) indicted that bubble populations over a depth of ~1 m control the enhanced infrared absorption, and for whitecaps, higher wind speeds cause more pronounced disruption of the water surface and entrainment of air to greater depths, causing a direct relationship between windspeed (or water disturbance) and near infrared absorption. For the ship wakes we present, at

distances removed from the stern (i.e. for portions of the wake which are "older") bubbles from the sub–layer will have had more time to dissipate, thus causing the visible to near infrared spectral slope to decrease. At higher speeds entrainment of air to depth will be enhanced. For the vessel we observed it appears that significant enhancement of the visible to near infrared reflectance slope occurred somewhere between speeds of ~7 and 11 m $s^{-1}$. In accordance with the findings of Zhang et al. (2004) we also find a subtle enhancement of reflectance in the 750–800 nm region, with the subtle reflectance peak visible in the wakes we present here (Figure 1) of 760 nm in direct correspondence to that reported by Zhang et al. (2004; Figure 2, therein).

Figure 2b shows how the spectral reflectance of the turbulent wake decays with distance aft of the vessel at three reference wavelengths: 523 nm, 695 nm, and 870 nm. These wavelengths were chosen as those at which the wake exhibited maximum reflectance, minimum reflectance, and a mid–point in–between. Reflectance is at a maximum immediately aft of the vessel. At this location (the proximal region of the wake) reflectance increases as vessel speed increases. Using the 523 nm reflectance (the reflectance maximum) as an index, the length of the turbulent wake (i.e. the distance aft of the ship that the wake is discernable in the image data) also increases as vessel speed increases (Figure 1 and Figure 2b). For the three wakes it is possible to estimate the time length of time for which the bubbles which constitute the turbulent wake persist (the age, or survival time of the bubbles/wake at a particular distance along its long axis), given that the speed of the vessel is known. At 3.6 m $s^{-1}$ reflectance falls to background levels within approximately 15 seconds after wake formation. At 7.2 and 10.8 m $s^{-1}$ the wake reflectance falls to background levels ~30 s and ~40 s, respectively.

Figure 2c shows how the spectral reflectance of the ship's wake varied across its long axis (here displaying profiles only for the visible blue and red wavelengths). For each vessel speed reflectance is plotted either side of the centerline of the wake, at proximal (immediately aft of the vessel), distal, and medial distances. The change in structure of the wake with increasing speed is apparent. For example, immediately aft of the vessel at 3.6 m $s^{-1}$ (Figure 2ciii) the wake is a single reflectance feature with a maximum reflectance of ~0.15. As vessel speed increases the wake reflectance increases (to ~0.8 at 10.8 m $s^{-1}$), and the wake becomes wider and more complex. By the time vessel speed has increased to 10.8 m $s^{-1}$ (Figure 2ci) the wake is clearly composed of three distinct foam bands; two lateral wake bands (of similar reflectance) with another located between these outer limbs characterized by a significantly lower reflectance (wash).

The data we have presented here were acquired from an airborne platform, to document the reflectance properties of the wake at high spatial (1.5 m), radiometric (12 bit), and spectral (60 bands) resolution. However, remote observation of ship wakes as a means of ship detection and maritime surveillance requires an appropriately high revisit period and an orbital solution (to provide repeated coverage over wide geographic areas). The corollary of higher temporal resolution and synoptic coverage afforded from low Earth orbit is lower spatial resolution. Figure 3 provides an example of how the how the ability to spectrally distinguish the wake from the adjacent background ocean decreases as spatial resolution decreases (i.e. becomes more coarse). A simple statistical t–test indicates that the wake depicted here (produced at a speed of 7.2 m $s^{-1}$) becomes statistically similar to the background ocean once spatial resolution exceeds ~30 m. Clearly wake size and reflectance is a function of vessel speed (as demonstrated here) and vessel size. Furthermore, the ability to distinguish a "wake" pixel from a "background" pixel depends on the dimensions of the wake relative to the spatial resolution of the sensor and it's reflectance (a more reflective sub–pixel–sized wake making a larger contribution to the at–sensor radiance than a less reflective wake of the same size). Nevertheless, spatial resolutions of decameters are easily attainable from small satellites. A constellation of small satellites could provide a maritime surveillance system capable of detecting and monitoring ship traffic in the open ocean, with the spatial resolution of desired inversely proportional to the number of spacecraft required.

## IV. Conclusions

Hyperspectral images of the United States Coast Guard Cutter Kittiwake, acquired by an airborne sensor, have been used to document the spectral reflectance of the turbulent wake produced by the vessel at three different speeds of 3.6 m $s^{-1}$ (low), 7.2 m $s^{-1}$ (medium), and 10.8 m $s^{-1}$ (high). The turbulent wake of the Kittiwake becomes longer, wider, more reflective (with an increasingly pronounced visible to near–infrared reflectance slope), and assumes a more complex plan form (two distinct wakes separated by a wash zone), as vessel speed increases. At a spatial resolution of 1.5 m, the wakes produced by this vessel disappear from the spectral record after ~15 s (3.6 m $s^{-1}$) to ~30 to 40 s (10.8 m $s^{-1}$) after foam formation.

## V. Figures Captions

Figure 1

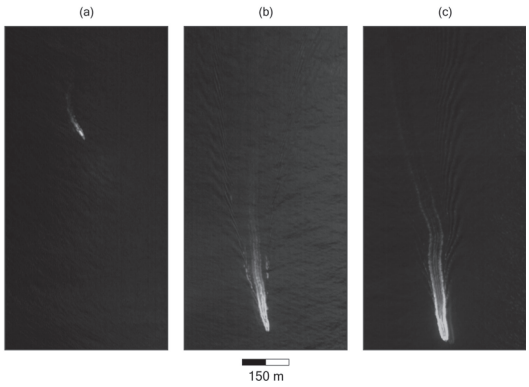


Figure 1. HICO images of the USCGC Kittihawke acquired off the west coast of Oahu, Hawai'i, on 8 April, 2010. Images (a), (b), and (c) show the wake generated by the Kittiwake at speeds of ~3.5 m $s^{-1}$ (7 knots), ~7 m $s^{-1}$ (14 knots) and 11 m $s^{-1}$ (21 knots). Image (d) shows the vessel at rest. Pixel size is approximately 1.5 m × 1.5 m.

Figure 2

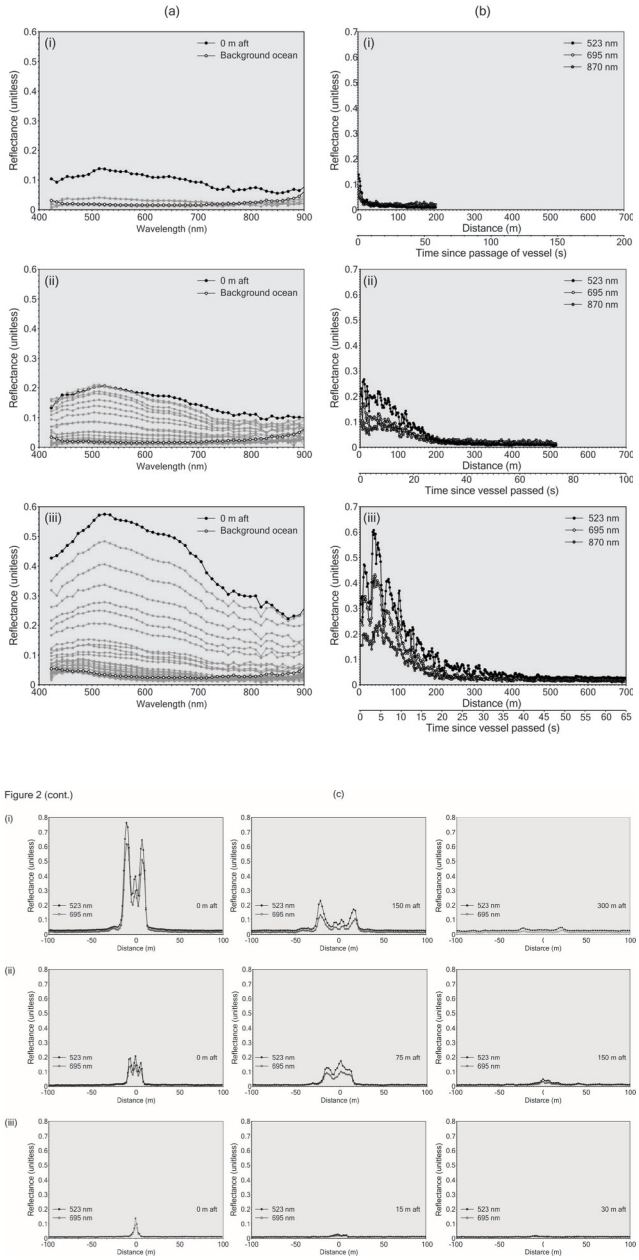


Figure 2 (cont.)




Figure 2. (a) Spectral reflectance of the wakes acquired at 15 m intervals from the stern to the point at which the wake became spectrally indistinct from the adjacent ocean, for speeds of ~3.5 m $s^{-1}$ (i), ~7 m $s^{-1}$ (ii) and ~11 m $s^{-1}$ (iii). (b) Spectral reflectance along the long axis of the turbulent wake at three wavelengths (523, 695, and 870 nm) for speeds of (i) ~3.5 m $s^{-1}$, (ii) ~7 m $s^{-1}$, and (iii) ~11 m $s^{-1}$. (c) Spectral reflectance across the turbulent wake at 523 and 695 nm, at the proximal, medial, and distal reaches of each wake (distances aft of the vessel at which the spectral profiles were extracted are noted on each chart).

Figure 3

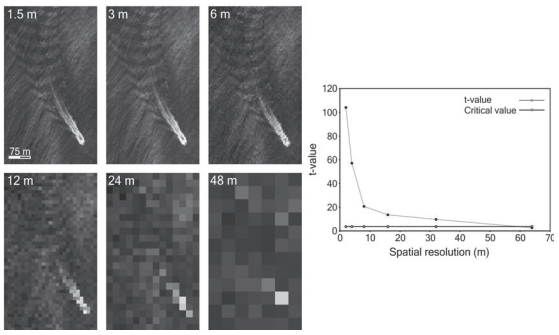


Figure 3. HICO image of the Kittiwake travelling at 7.2 m $s^{-1}$. The raw 1.5 m data have been resampled using nearest neighbor technique. The chart on the right shows how the spectral reflectance of the wake at 523 nm becomes increasingly subdues as spatial resolution decreases.

## REFERENCES


[1] Berk, A., Bernstein, L.S., and Robertson, D.C., (1989). MODTRAN: A Moderate Resolution Model for LOWTRAN7, Rep. GL–TR–89–0122, Air Force Geophys. Lab., Bedford, MA.

[2] Eldhuset, K., (1999). An automatic ship and ship wake detection system for spaceborne SAR images in coastal regions. *IEEE Trans. Geo. and Remote Sensing*, **34**, 1010–1019.

[3] Frouin, R., Schwindling, M., and Deschamps, P–Y., (1996). Spectral reflectance of sea foam in the visible and near–infrared: in situ measurements and remote sensing implications. *J. Geophys. Res.*, **101**, 14,361–14,371.

[4] Hennings, I., Romeiser, R., Alpers, W., and Viola, A (1999). Radar imaging of Kelvin arms of ship wakes. *Int. J. Remote Sensing*, **20**, 2519–2543.

[5] McGlynn, J.D., Stewart, S.R., and Witte, D.J., (1990). Advances in sensing and detection of thermal infrared ship wakes. Presented at *Oceans' 90: Engineering in the Ocean Environ –ment*, Washington D.C., 1990, 24–26 September 1990.

[6] Munk, W.H., Scully–Power, P., and Zacharisen, F., (1987). Ships from space. *Proc. R. Soc. Lond. A*, **412**, 231–254.

[7] National Defense Research Committee, (1989). *Physics of Sound in the Sea*. Peninsula Publishing, Los Altos, CA. 577 pp.

[8] Reed, A.M., and Milgram, J.H., (2002). Ship wakes and their radar images. *Annu. Rev. Fluid. Mech.*, **34**, 469–502.

[9] Stabeno, P.J., and Monahan, E.C., (1986). The influence of whitecaps on the albedo of the sea surface, in *Oceanic Whitecaps*, edited by E.C. Monahan and G.M. Niocaill, pp. 261–266, D. Reidel, Norwell, Mass.

[10] Thompson, W., (1887). On ship waves. *Proc. Instn. Mech. Engrs.*, pop. lect., p. 482.

[11] Trevorrow, M.V., Vagle, S., and Farmer, D.M., (1994). Acoustical measurements of microbubbles within ship wakes. *J. Acoust. Soc. Am.* **95**, 1922–1930.

[12] Zhang, X., Lewis, M., Bissett, W.P., Johnson, B., and Kohler, D., (2004). Optical influence of ship wakes. *Appl. Opt*., **43**, 3122–3132.